# Creation of Faceted Polyhedral Microgels from Compressed Emulsions

*Jing Fan, Shin-Hyun Kim,* Zi Chen, Shaobing Zhou, Esther Amstad, Tina Lin, and David A. Weitz**

*Compressed monodisperse emulsions in confined space exhibit highly ordered structures. The influence of the volume fraction and the confinement geometry on the organized structures is investigated and the mechanism by which structural transition occurs is studied. Based on the understanding of ordering behavior of compressed emulsions, a simple and high-throughput method to fabricate monodisperse polyhedral microgels using the emulsions as the template is developed. By controlling the geometry of the confined spaces, a variety of shapes such as hexagonal prism, Fejes Toth honeycomb prism, truncated octahedron, pyritohedron, and truncated hexagonal trapezohedron are implemented. Moreover, the edge sharpness of each shape is controllable by adjusting the drop volume fraction. This design principle can be readily extended to other shapes and materials, and therefore provides a useful means to create polyhedral microparticles for both fundamental study and practical applications.*

Prof. J. Fan
Department of Mechanical Engineering
The City College of New York
New York, NY 10031, USA
Prof. S.-H. Kim
Department of Chemical and Biomolecular Engineering
KAIST
Daejeon 34141, Republic of Korea
E-mail: kim.sh@kaist.ac.kr
Prof. Z. Chen
Thayer School of Engineering
Dartmouth College
Hanover, NH 03755, USA
Prof. S. Zhou
School of Materials Science and Engineering
Key Laboratory of Advanced Technologies of Materials
Southwest Jiaotong University
Chengdu, 610031 Sichuan, China
Prof. E. Amstad
EPFL-STI-IMX-SMAL
MXC 230, Station 12, CH-1015 Lausanne, Switzerland
Dr. T. Lin, Prof. D. A. Weitz
Department of Physics and School of Engineering and Applied Sciences
Harvard University
Cambridge, MA 02138, USA
E-mail: weitz@seas.harvard.edu

DOI: 10.1002/smll.201701256

## 1. Introduction

Microparticles with diverse shapes have been widely used in fundamental research on self-assembly, jamming transition, rheology of particulate systems, transport behavior of particles through narrow channels, and property–structure relationship in materials.[1] Moreover, shape-controlled hydrogel microparticles are promising for many practical applications due to their unique biochemical and mechanical properties, serving as delivery carriers for drugs and building blocks for engineered tissue scaffolds.[1a,2] In many circumstances, particle shape is a critical determinant of the function and self-assembly behavior of the particles. Despite the significance of particle shape, however, relevant studies on the shape effect are still limited due to the technical difficulty in designing hydrogel particles with nonspherical 3D geometries. Although recent advances in flow lithography, imprint lithography, and microfluidic technology have enabled the creation of hydrogel particles with nonspherical shapes, the particles are usually lithographically featured or individually molded by the geometry of microchannel, restricting to 2D extruded shapes.[1a,3] The more recent liquid bridge method and capillary origami method enable the fabrication of microgels with complex 3D shapes; however, the throughput of these methods could still be improved.[4] Simple and high-throughput fabrication of microgels with truly 3D

  

shapes, especially the representative shapes of polyhedra, would benefit fundamental studies in areas such as self-assembly, the jamming transition, and the rheology of particulate systems.

Dispersion systems of two immiscible fluids with mobile interfaces exhibit a rich variety of self-organized structures in which the dispersed phase forms truly 3D building blocks. For example, monodisperse bubbles or drops deform to be non-spherical cells and form regular lattice when they are highly concentrated in a continuous-phase liquid. The resultant foams or emulsions have also served as a model system to study the long-standing problem of seeking the structure with minimum surface area to partition a space into equal-volume cells; this has intrigued mathematicians, physicists, and engineers for centuries.[5] In nature, the honeycomb constructed by bees represents a dispersion system with natural pattern formation in which uniform air cavities form hexagonal arrays with the minimum wall area. Evidence has been recently found from a beehive under construction that the formation of such an efficient structure should be credited more to surface tension rather than the skill of bees; surface tension pulls the circular cavities into hexagonal during the consolidation of wax.[6]

Inspired by these studies, we develop a simple and high-throughput method to create hydrogel microparticles with quasi-polyhedral shapes using compressed emulsions as the template. Dispersed drops squeeze against each other when they are compressed above the densest packing for spheres. More importantly, the drops form a regular lattice composed of uniform polyhedrons. We can realize a variety of shapes by adjusting the confining geometry and the drop volume fraction; the polyhedral drops then serve as a microparticle template. To implement this system, we use microfluidic devices to prepare monodisperse water drops in a continuous oil phase; the drops contain photo-crosslinkable hydrogel precursors and are confined between two parallel plates. As the volatile continuous phase is depleted by vaporization, the water drops become highly compressed, gradually turning faceted to form quasi-polyhedrons. Photopolymerization of hydrogel precursors freezes the shape of the deformed drops and yields uniform quasi-polyhedral hydrogel particles. With two parallel flat plates accommodating a monolayer of drops, we obtain circular and hexagonal discs/prisms; with two parallel flat plates accommodating a double layer of drops, we obtain Fejes Toth honeycomb prisms;[7] and with two parallel flat plates accommodating a multilayer of drops, we obtain truncated octahedrons.[5] Using two plates with a simple post array, we further realize the Weaire–Phelan packing structure that results in pyritohedron and truncated hexagonal trapezohedron particles.[8] This approach features simplicity and high yield and can be extended to other polyhedral shapes and materials, providing new opportunities for the study of shape effect in both fundamental research and practical applications.

## 2. Results and Discussion

### 2.1. Experimental Generation of Microgels

Monodisperse water-in-oil (W/O) emulsion drops are produced using glass capillary microfluidic devices.[9] The dispersed phase is an aqueous solution of 10 wt% poly(ethylene glycol) diacrylate (PEGDA, Mw 700) containing 0.1 wt% Irgacure 2959 as a photoinitiator. The continuous phase is a volatile fluorocarbon oil (HFE-7500) with 1 wt% Krytox-PEG surfactant.[10] While generating the drops, we match the volumetric flow rates of the dispersed phase with the continuous phase, resulting in an initial drop volume fraction of 0.5. We collect the drops in chambers consisting of two parallel plates. The distance between the two plates is controlled by spacers with different thicknesses, varying from 0.04 to 4 mm. The lateral dimension of the chambers is 20–50 mm. For chambers thinner than 0.4 mm, we place the chamber horizontally and seal two opposite sides with spacers and epoxy, leaving the other two sides open for evaporation of the continuous phase. For chambers thicker than 0.4 mm, we seal three sides of the chamber and place the chamber vertically with the top side open. As the continuous phase evaporates, the drop volume fraction increases from the initial value of 0.5 to almost 1. During this process, the drops gradually pack to lattice structures and may change their packing structure multiple times; each individual drop gradually deforms to a polyhedral shape with increasing edge sharpness. When the closely packed drops form the target or exhibit the target edge sharpness, we polymerize them by shining 365 nm UV light with an intensity of 0.4 mW $cm^{-2}$ for 10 min. In the course of polymerization, the drops do not change their packing structure. The resultant hydrogel particles are subsequently dispersed into deionized water.

### 2.2. Drop Packing in Flat-Plate Chambers and Resultant Microgels

We first examine the packing structure within the flat-plate chambers. The packing structure depends on the drop volume fraction $\phi$ and the nondimensional chamber thickness $\varepsilon$, defined as the ratio of the chamber thickness to the initial drop diameter. For each value of $\varepsilon$ we inspect the structural evolution as $\phi$ increases. With increasing $\phi$, the edges of the polyhedra become sharper and the packing of the structure can undergo a transition to a new structure. With increasing $\varepsilon$, the chamber can accommodate more layers of drops.

#### *2.2.1. Single-Layer Drop Packing and Resultant Microgels*

When $\varepsilon$ is smaller than or comparable to 1, only one layer of drops can pack between the two plates. It forms a 2D hexagonal close packing structure following partial evaporation of the continuous phase (**Figure 1**a). As the continuous phase further evaporates, the drops squeeze each other and adopt the shape of a hexagonal prism, as shown in Figure 1b,c. By polymerizing the deformed drops at different volume fractions, we fabricate hexagonal-prism particles with different edge sharpness, as shown in Figure 1d–f. Moreover, by adjusting the chamber thickness, we can control the shape from flat discs to tall prisms, as shown in Figure 1g.

  

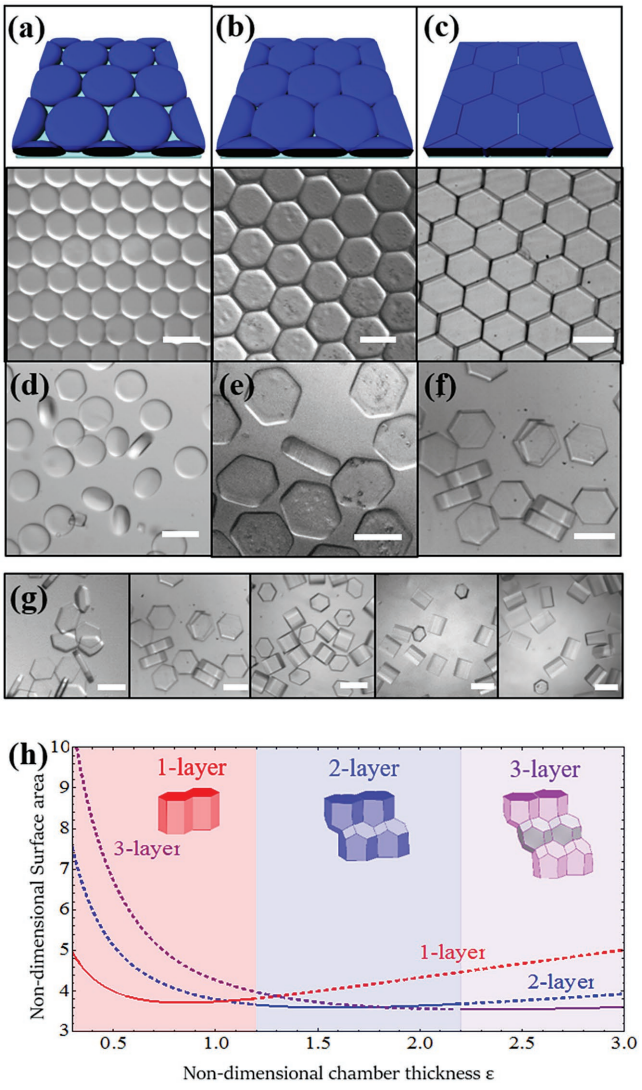


**Figure 1.** Schematics and microscopy images of hexagonal packing of drops at three volume fractions: a) 70–80%, b) 80–90%, and c) >90%. d–f) Microscopy images of the corresponding microgels with different edge sharpness; the microgels are dispersed in water. g) Hexagonal prism microgels of different aspect ratios. h) Curves represent the average surface area of one unit deformed from a spherical drop with a diameter of 1 in monolayer, double-layer, and triple-layer structures; for the triple-layer structure, the surface area comes from the average of two boundary units and one middle-layer unit. The red, blue, and purple regions illustrate the range of $\varepsilon$ for monolayer, double-layer, and triple-layer structures in experiments. All scale bars are 200 µm.

### *2.2.2. Double-Layer Drop Packing, Structural Transition, and Resultant Microgels*

As $\varepsilon$ increases further, the drops can transition to double-layer packing at a higher $\phi$ even if they pack into a single layer at the initial volume fraction. The larger the $\varepsilon$, the more layers of drops the chamber can accommodate at $\phi$ close to 1. To determine if the structure of the compressed emulsion at $\phi$ close to 1 is driven by surface energy, we first experimentally find the values of $\varepsilon$ at which the structure transforms from monolayer to double-layer and from double-layer to triple-layer.[11] We collect monodisperse drops in a wedged chamber with a slope of 0.004 and wait until the continuous oil fully evaporates (Figure S1, Supporting Information). We find that the drops pack into the monolayer structure when $\varepsilon$ is smaller than 1.2, double-layer when $\varepsilon$ is between 1.2 and 2.2, and triple-layer when $\varepsilon$ is larger than 2.2; the red, blue, and purple regions in Figure 1h illustrate this result. To determine if the structures observed correspond to the lowest surface energy, for each of the three structures we calculate the average surface area of one unit deformed from a spherical drop with a diameter of 1 over the range of $\varepsilon$ from 0.3 to 3.0 and at $\phi = 1$. The monolayer structure has the lowest surface energy when $\varepsilon$ is smaller than 1.05; the double-layer structure has the lowest surface energy when $\varepsilon$ is between 1.05 and 1.8; and the triple-layer structure has the lowest surface energy when $\varepsilon$ is larger than 1.8 (Figure 1h). The slight discrepancy between experiment and calculation arises because the calculation does not consider the deformation-induced energy barrier that the drops have to overcome to rearrange themselves at the boundaries between lattices of different layer thicknesses.

The double-layer packing of drops exhibits two distinct structures during drainage. At relatively low $\phi$, the structure is a beehive honeycomb, in which each layer of drops forms a hexagonal packing, and each drop is located in the middle of the triangle formed by three touching drops from the other layer, as shown in **Figure 2**a. As $\phi$ further increases, the beehive structure slips by a half lattice constant to form the structure shown in Figure 2b; this structure was first discussed by Fejes Toth in 1964.[7] In the Fejes Toth structure each layer of drops still forms a hexagonal packing, but each drop is located in the middle of four touching drops from the second layer. Therefore, each deformed drop has 11 faces: one flat hexagon that contacts the chamber plate, six faces that are shared with six neighboring drops in the same layer, and four additional faces formed by two squares and two hexagons that are shared with four neighboring drops in the second layer, as indicated by the inset of Figure 2b. Except for the six edges of the flat hexagon, all the other edges are slightly curved so that every four edges meet at one vertex with the angle of 109.47° to satisfy the mechanical equilibrium, while maintaining zero mean surface curvature. This structure conforms to the Plateau laws that describe the structure of emulsions at very high volume fraction.[12] Therefore, the Fejes Toth hexagonal prism is quasi-faceted.

To understand how $\phi$ influences the double-layer packing structure, we examine the drop packing at 16 independent regions of interest over a wide range of $\phi$; each region of interest contains about 1000 drops with a diameter of 56 µm and packed between an 84 µm thick chamber, as shown in Figure S2 (Supporting Information). For each region we measure the fraction of drops in the beehive honeycomb and the Fejes Toth honeycomb, respectively; there is also a small amount of drops at the grain boundaries showing neither the beehive nor the Fejes Toth honeycomb structure. We estimate the value of $\phi$ based on the drop size, number, area of the region of interest, and chamber thickness, and then plot the fractions of drops in different structures as a function of $\phi$. The results show that when the drop volume fraction is less

  

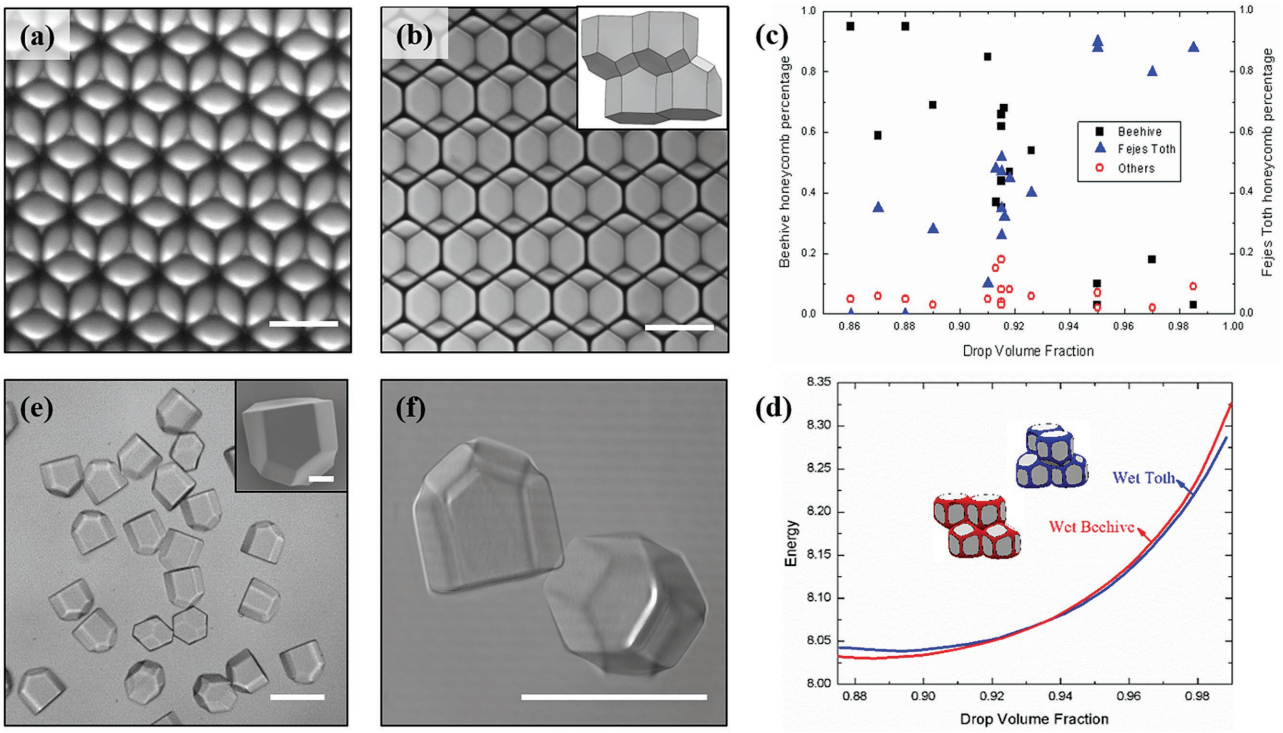


**Figure 2.** Microscopy images of double-layer packing at low and high volume fractions, showing a) beehive honeycomb and b) Fejes Toth honeycomb structures, respectively. c) Fractions of drops in beehive and Fejes Toth honeycomb structures as a function of drop volume fraction with drop diameter of 56 μm at $\varepsilon = 1.5$. d) Nondimensional interfacial energy of beehive and Fejes Toth honeycomb structures at $\varepsilon = 1.5$. e,f) Microscopy images of Fejes Toth prism microgels with SEM image as the inset. Inset scale bar is 20 μm; all other scale bars are 200 μm.

than ≈0.915, the beehive honeycomb structure dominates, otherwise the Fejes Toth structure dominates (Figure 2c).

Surprisingly, this transition volume fraction varies with the drop size even if $\varepsilon$ remains the same, although the interfacial energy depends solely on $\varepsilon$ at a given volume fraction. For example, when $\varepsilon = 1.5$, the packing structure of 250 μm diameter drops undergoes a transition at a volume fraction of ≈0.85 whereas the packing structure of 180 μm diameter drops undergoes a transition at ≈0.89 (Movie S1, Supporting Information); both of these are much smaller than the value of 0.915 at which 56 μm diameter drops undergo a packing transition. This indicates that there is another factor contributing to the structural transition besides interfacial energy.

To determine the other contributing factor, we calculate the nondimensional interfacial energy for the beehive and Fejes Toth honeycomb structures at $\varepsilon = 1.5$ using the Surface Evolver, as shown in Figure 2d.[13] The nondimensional interfacial energy arises from two units deformed from spherical drops with a diameter of 1 and with an interfacial tension of 1; we neglect the film thickness and the difference of interfacial tension between films and Plateau borders.[14] This calculation predicts a transition volume fraction of ≈0.935: when the drop volume fraction is smaller than 0.935, the beehive honeycomb structure is energetically favorable, otherwise the Fejes Toth honeycomb structure is favorable. However, our experiments show that the beehive honeycomb structure transitions to the Fejes Toth honeycomb at volume fractions much lower than 0.935, implying that the beehive structure is less stable than the Fejes Toth structure for some range of volume fraction. Indeed, the beehive structure possesses eightfold vertices that violate the fourfold vertex requirement of the Plateau law, and therefore is not mechanically stable. It is noteworthy that the energy difference between the beehive honeycomb and Fejes Toth honeycomb is small: <0.15% for drop volume fraction between 0.85 and 0.935.

The drop size-dependence of the transition volume fraction can be explained by the disturbance-triggered instability of the beehive honeycomb structure. Consider two chambers accommodating different sized drops but with the same nondimensional chamber thickness. The one containing larger drops has a larger opening, and thus yields faster evaporation of the continuous phase. For example, for drops larger than 100 μm, it takes less than 30 min to fully evaporate the continuous phase; while for drops with a diameter of 56 μm, it takes ≈3 h. Fast evaporation induces sufficient disturbance to trigger the transition from the unstable beehive structure to the more stable Fejes Toth structure. By contrast, with slow evaporation, the beehive structure persists over a wider range of volume fractions.

With drops larger than 100 μm we exclusively achieve the Fejes Toth honeycomb structure after evaporating most of the continuous phase; this yields uniform hydrogel particles in the shape of Fejes Toth honeycomb prisms, as shown in Figure 2e,f. The particles keep their original shapes when they are fully dehydrated, as confirmed by the scanning electron microscopy (SEM) image in the inset of Figure 2e.

  

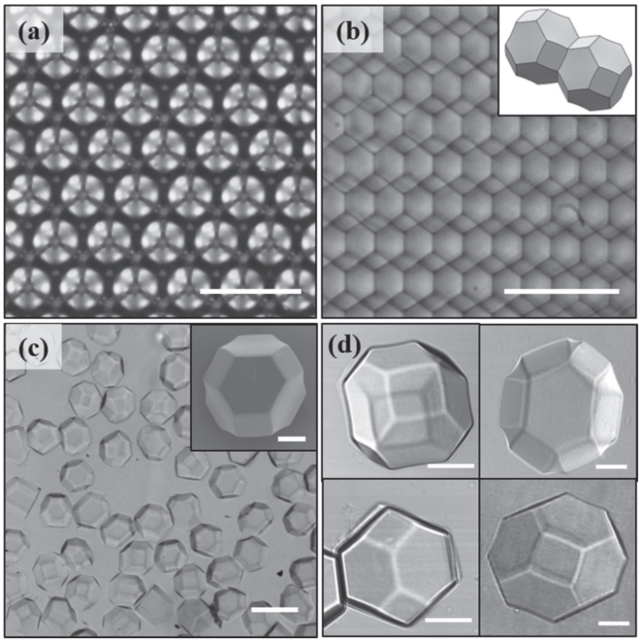


**Figure 3.** Microscopy images of a) FCC packing and b) BCC packing of multilayer drops confined in thick chambers. c,d) Microscopy images of the resultant microgels with Kelvin structure; inset of (c) is the SEM image of a dried microgel. Scale bars are 200 μm in (a)–(c), 50 μm in (d), and 20 μm in the inset of (c).

*2.2.3. Multilayer Drop Packing and Resultant Microgels*

Similar to the double-layer packing, multilayer packings exhibit two different structures depending on the drop volume fraction. At relatively low volume fractions, drops form face-centered-cubic (fcc) or hexagonal close packing (hcp) structures as shown in **Figure 3**a; this is also the densest packing structure of hard spheres. As $\phi$ gets closer to 1, the drops pack into a body-centered-cubic (bcc) structure, as shown in Figure 3b; the drops next to the flat plates are Fejes Toth hexagonal prisms whereas those in the middle layers have a Kelvin structure.[5] Each Kelvin unit looks like a truncated octahedron with six flat square faces and eight hexagonal faces of a monkey-saddled shape, conforming to the Plateau law, as shown schematically in the inset of Figure 3b. Movie S2 (Supporting Information) shows the packing structure with seven layers of drops, in which the focal plane is gradually adjusted from the first layer to the seventh layer. The resultant hydrogel particles are shown in Figure 3c,d. Using a 4 mm thick chamber with a nondimensional chamber thickness of 27 which accommodates more than 30 layers of drops, all layers exhibit the bcc structure, despite some defects and distortion. This allows us to fabricate ≈1 million truncated octahedron hydrogel particles at once.

### 2.3. Drop Packing in Patterned-Template Chambers and Resultant Microgels

To further extend the variety of achievable geometries, we apply a patterned template to facilitate forming other packing structures. As a proof of concept, we target the Weaire–Phelan structure, which is known to have the minimum surface area for partitioning a space into equal volumes.[8] This implies that a compressed emulsion with a drop volume fraction of 1 should form Weaire–Phelan structure in unlimited space; its interfacial energy is 0.3% lower than that of the Kelvin structure. The unit cell of the Weaire–Phelan structure consists of eight equal-volume blocks as shown in **Figure 4**a; six of the eight blocks are truncated hexagonal trapezohedrons with 12 pentagonal and two hexagonal faces

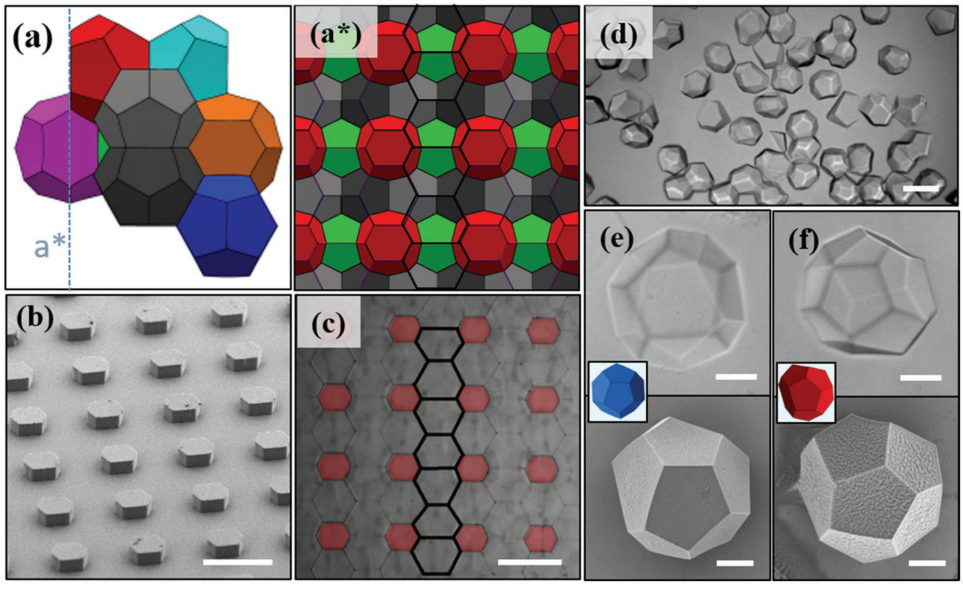


**Figure 4.** a) Schematics of the unit cell of Weaire–Phelan structure; a*) cross section of Weaire–Phelan structure at the boundary marked by the dashed line in (a). b) SEM image of the patterned template. c) Microscopy image of drop packing on the surface of template. d–f) Microscopy and SEM images of dodecahedron and tetrakaidecahedron microgels. Scale bars are 200 μm in (b)–(d), 50 μm in the optical images of (e) and (f), and 20 μm in the SEM images of (e) and (f).

  

and the other two are pyritohedrons. Looking from left to right at the cross section marked with the dashed line in Figure 4a and neglecting the halved blocks, we see the plane in Figure 4a* in which the light gray, dark gray, and green blocks are in the same layer, forming a relatively flat surface, while the red blocks form bumps. Thus in flat-plate chambers, we cannot realize the Weaire–Phelan structure because it is incompatible with flat boundaries.[15]

We instead design the chamber plates with a square array of hexagonal posts whose periodicity is the lattice constant of Weaire–Phelan structure, as shown in Figure 4b. The periodicity and size of the hexagons are the same as the red hexagonal faces in Figure 4a*; the height is chosen to hold a half volume of the boundary-layer blocks beneath the posts. We align the two plates under a microscope and control their distance with spacers to match the lattice. After filling the chamber with drops and evaporating almost all continuous phase, the drops deform and pack into the Weaire–Phelan structure. The arrangement of drops in the boundary layer is shown by Figure 4c, in which the posts on the template have been marked in red for better visualization. Movie S3 (Supporting Information) reveals the packing structure up to the fifth layer, in which the focal plane gradually moves farther from the boundary layer. As evidenced by both Figure 4c and Movie S3 (Supporting Information), although the template does not provide exact guidance for each individual drop, the drops can still successfully pack into the Weaire–Phelan structure due to its low interfacial energy. The resultant polyhedral hydrogel particles are shown in Figure 4d. These particles consist of two distinct unit blocks in pyritohedronal and tetradecahedronal shapes; the latter is a truncated hexagonal trapezohedron. Figure 4e,f shows the optical microscope and SEM images of each shape. Similar to the Kelvin structure and the Fejes Toth prism, they are quasi-faceted polyhedrons in which the faces are slightly curved except for the two hexagonal faces in the tetradecahedron.

## 3. Conclusion

In summary, a facile and effective approach to fabricate polyhedral hydrogel microparticles is demonstrated by confining monodisperse emulsion drops in between two parallel plates at a high volume fraction and polymerizing the deformed drops by UV irradiation. Using flat plates, we create hexagonal discs and prisms, Fejes Toth honeycomb prisms, and truncated octahedron particles by adjusting the ratio of the distance between the two plates to the drop size. Using a guiding micropattern with a square array of hexagonal posts that have the same lattice constant as the Weaire–Phelan structure, we also create pyritohedron and truncated hexagonal trapezohedron particles. We expect that the achievable geometries could be further extended by the same strategy; for example, the 15-hedra and 16-hedra shapes in periodic tetrahedrally close-packed structures might be produced.[16] A similar method can be applied to other polymerizable materials as well. The achievable size of the polyhedral particles is on the order of 10 μm to 1 mm. The resultant polyhedral microgels can potentially provide useful building blocks for the fundamental study of self-assembly; moreover, they may have practical applications in tissue engineering. This approach also represents an effective method to investigate a spectrum of physical and mathematical problems, such as crystal structures, defects, phase transition, jamming, and minimum surface area.

## Supporting Information

*Supporting Information is available from the Wiley Online Library or from the author.*

## Acknowledgements

*J.F. and S.-H.K. contributed equally to this work. This work was supported by the Harvard Materials Research Science and Engineering Center (DMR-1420570) and the National Science Foundation (DMR-1310266). J.F. appreciates the support from the Advanced Energy Consortium. S.-H.K. appreciates partial support from Global Research Laboratory (NRF-2015K1A1A2033054) through the National Research Foundation Korea (NRF). Z.C. acknowledges the support by the Society in Science-Branco Weiss Fellowship, administered by ETH Zürich.*

## Conflict of Interest

*The authors declare no conflict of interest.*

[1] a) D. Dendukuri, P. S. Doyle, *Adv. Mater.* **2009**, *21*, 4071; b) S. Mukhopadhyay, J. Peixinho, *Phys. Rev. E* **2011**, *84*, 011302; c) M. Cloitre, R. Borrega, L. Leibler, *Phys. Rev. Lett.* **2000**, *85*, 4819; d) R. Haghgooie, M. Toner, P. S. Doyle, *Macromol. Rapid Commun.* **2010**, *31*, 128; e) A. G. Athanassiadis, M. Z. Miskin, P. Kaplan, N. Rodenberg, S. H. Lee, J. Merritt, E. Brown, J. Amend, H. Lipson, H. M. Jaeger, *Soft Matter* **2014**, *10*, 48.
[2] a) J. A. Champion, Y. K. Katare, S. Mitragotri, *J. Controlled Release* **2007**, *121*, 3; b) G. Eng, B. W. Lee, H. Parsa, C. D. Chin, J. Schneider, G. Linkov, S. K. Sia, G. Vunjak-Novakovic, *Proc. Natl. Acad. Sci. USA* **2013**, *110*, 4551.
[3] a) D. Dendukuri, D. C. Pregibon, J. Collins, T. A. Hatton, P. S. Doyle, *Nat. Mater.* **2006**, *5*, 365; b) J. P. Rolland, B. W. Maynor, L. E. Euliss, A. E. Exner, G. M. Denison, J. M. DeSimone, *J. Am. Chem. Soc.* **2005**, *127*, 10096.
[4] a) L. Wang, M. Qiu, Q. Yang, Y. Li, G. Huang, M. Lin, T. J. Lu, F. Xu, *ACS Appl. Mater. Interfaces* **2015**, *7*, 11134; b) M. Li, Q. Yang, H. Liu, M. Qiu, T. J. Lu, F. Xu, *Small* **2016**, *12*, 4492.
[5] D. Weaire, *The Kelvin Problem: Foam Structures of Minimal Surface Area*, Taylor & Francis, Bristol, PA **1996**.
[6] P. Ball, *Nature News* **2013**, DOI: 10.1038/nature.2013.13398.
[7] L. F. Toth, *Bull. Am. Math. Soc.* **1964**, *70*, 468.
[8] D. Weaire, P. Phelan, *Philos. Mag. Lett.* **1994**, *69*, 107.
[9] A. S. Utada, E. Lorenceau, D. R. Link, P. D. Kaplan, H. A. Stone, D. A. Weitz, *Science* **2005**, *308*, 537.

  

[10] C. Holtze, A. C. Rowat, J. J. Agresti, J. B. Hutchison, F. E. Angile, C. H. J. Schmitz, S. Koster, H. Duan, K. J. Humphry, R. A. Scanga, J. S. Johnson, D. Pisignano, D. A. Weitz, *Lab Chip* **2008**, *8*, 1632.
[11] W. Drenckhan, S. Hutzler, *Adv. Colloid Interface* **2015**, *224*, 1.
[12] J. E. Taylor, *Ann. Math.* **1976**, *103*, 489.
[13] K. A. Brakke, *Exp. Math.* **1992**, *1*, 141.
[14] M. P. Aronson, H. M. Princen, *Nature* **1980**, *286*, 370.
[15] R. Gabbrielli, A. J. Meagher, D. Weaire, K. A. Brakke, S. Hutzler, *Philos. Mag. Lett.* **2012**, *92*, 1.
[16] J. M. Sullivan, in *Proc. Eurofoam 2000 Foams, Emulsions and their Applications*, Verlag MIT, Delft **2000**, p. 111.

Received: April 19, 2017
Revised: May 14, 2017
Published online:

  